Electrical, Control and Communication Engineering
ISSN 2255-9159 (online)
ISSN 2255-9140 (print)
2022, vol. 18, no. 1, pp. 1–10
https://doi.org/10.2478/ecce-2022-0001
https://content.sciendo.com

Dual-Band, EBG-DGS Wearable Antenna for Emergency Services and Responses in WBAN

Sandhya Mallavarapu* (*National Institute of Technology, Warangal, Telangana, India*),
Anjaneyulu Lokam (*National Institute of Technology, Warangal, Telangana, India*)

***Abstract* – The paper introduces a compact, thin flexible textile antenna integrated with an Electromagnetic Bandgap (EBG) and Defected Ground Structure (DGS) covering the Wireless Local Area Networks (WLAN) bands (2.4-2.485 GHz and 5.1-5.9 GHz) for emergency services and responses. The geometry and configuration of the proposed antenna are made from common clothing jeans fabric, which makes the antenna more flexible, thin, and conformal. A new configuration of EBG structure is developed using Minkowski fractal geometry as base geometry and a DGS with the complementary dumbbell-shaped slot to operate in WLAN standards. The EBG structure is used to isolate the antenna from the human body, whereas the DGS is used to improve the bandwidth and polarization purity. The prototype covers the WLAN bands with gains of 3.37 dBi and 6.47 dBi, a bandwidth of 115.9 MHz, and 398.06 MHz for the specified wireless bands. The integrated antenna demonstrates a Front to Back Ratio (FBR) of 16.77 dB and 32.72 dB, the radiation efficiency of 36.9 % and 73.8 %, and a better cross-polarization level at 2.45 GHz, 5.85 GHz, respectively. The antenna shows a high gain and an efficiency of about 70 % under the various bending scenario. Thus, the anticipated antenna is the most appropriate and potential candidate for wearable applications in various domains.**

***Keywords* – Defected ground structure (DGS), electromagnetic bandgap (EBG) substrates, emergency search services, internet of things (IoT), wearable antenna, wireless body area network (WBAN), wireless local area network (WLAN).**

I. Introduction

In today's era, wireless and wearable systems attract the most attention being a part of everyone's life. In this regard, wearable systems are considered advantageous in remote health care monitoring, smart clothing for front-line workers, radio tagging for childcare, transport, and emergency search services [1]. Ultimately, these wearable systems pinpoint the location of the wearer. The systems gather the data from on-body devices and collectively transmit the user data to the external rescue or data analysis centers. Here the antenna plays a paramount role in designing wearable units used in these services for transmitting/receiving the analysed data. Especially, multi-band antennas are required for easy exchange of data to other on-body devices and the base stations. As the demand for multi-functional devices increases day by day, significant elements such as antennas are expected to be more prominent in performance with multiple functionalities. The dual-band operation can be achieved with the advantage of cutting slots on the planar microstrip antenna [2], [3]; microstrip antenna loaded with shortening pins, parasitic patch elements [4], and some other techniques [5], [6] have been proposed and demonstrated by researchers. In practical situations, cutting slots on the radiating elements results in loss of conductor, i.e. less Q, which tends to improve the impedance bandwidth, and miniaturise the antenna. As the small size antennas have less efficiency and gain, there should be a limit/trade-off between bandwidth and gain of the antenna. On the other hand, embedding the shortening pins and parasitic patches cannot be suitable in the aspect of comfort and size for wearable applications. Yet, these methods have limited bandwidth, led to low gain, and less efficiency.

Electromagnetic Bandgap (EBG) planes are utilised at the back of the monopole antenna to achieve the required gain and efficiency. The EBG structures offer high impedance and prevent surface wave propagation inside the substrate for certain frequencies [7], [8]. On the other hand, the integrated antennas with EBG become too thick, large in size, and sometimes are less efficient with a low Front-to-Back Ratio (FBR) [9]–[11]. To further improve the isolation and radiation features of the flexible antenna, a novel method of integrating the antenna with an array of EBG unit cells and an etched Defective Ground Structure (DGS) at the backplane of EBG is utilised [12]. The EBG not only improves the isolation but also diminishes the effect of electromagnetic exposure to the human body. The DGS improves cross-polarization and co-polarization by changing the fields in the ground plane at the back of EBG.

In this paper, a dual-band monopole antenna is implemented on a jeans substrate by a U-shaped monopole configuration, backed by an EBG plane to enhance the gain and radiation characteristics. Further, the gain and isolation are improved by etching slots in the ground plane of EBG. The anticipated antenna is much thinner and low in volume than the reported models earlier. Also, it not only improves the antenna gain but also removes frequency offset. Prototypes are fabricated, assembled properly, and measured for the radiation

* Corresponding author.
E-mail: sandhyamallavarapu@student.nitw.ac.in

characteristics. Therefore, the anticipated wearable antenna was found to be a possible candidate for emergency search services.

The remaining paper is organised as follows: Section 2 discusses the design of monopole antenna; geometrical evolution of EBG and DGS; Section 3 refers to the performance and experimental verification of EBG-DGS integrated antenna in free space and deformed situations followed by conclusions in Section 4.

II. Design and Configuration

The antenna and the electromagnetic bandgap structures are designed and simulated using the software CST MW Studio 2019, whose method of operation depends on Finite Difference Time Domain (FDTD) techniques.

A. The Geometry of the Dual-Band Antenna

The dual-band nature of the proposed monopole antenna on a flexible substrate can be investigated utilising the brunching technique [13]. The fabricated antenna has two parts of U-shaped radiators on the top of the substrate and a partial ground plane at the bottom of the substrate, as shown in Fig. 1a. The adhesive copper film of thickness of 0.06 mm is used for the radiating parts and the ground plane. The larger U-shaped radiator resonant at 2.45 GHz and the smaller U-shaped radiator independently resonate at 5.85 GHz. The antenna is mounted on a low-cost, flexible jeans substrate, having a dielectric constant of 1.7 and thickness of 0.7 mm. A 50 Ω microstrip line is employed to excite the monopole antenna in the middle of the U shape. The dual-band is achieved with appropriate dimensions of the top and lower U-shaped patches, the space between them, and also the extent of the ground plane. All the dimensions are obtained and optimized with the parametric simulations conducted in CST Microwave studio.

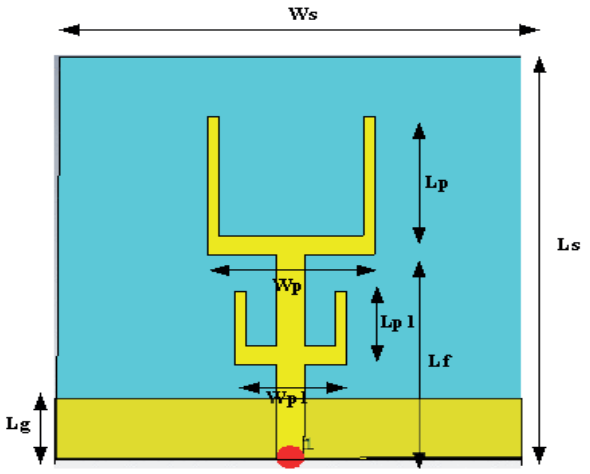

(a)

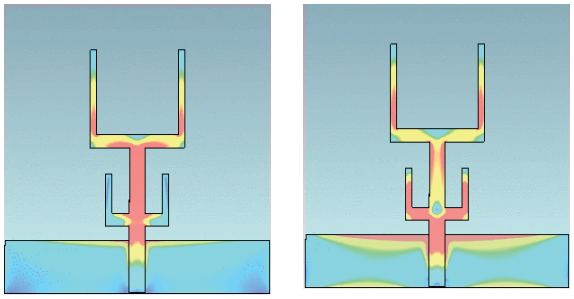

(b) (c)

Fig. 1. (a) Geometry; (b) Current distributions at 2.45 GHz; (c) Current distributions at 5.8 GHz of the anticipated dual-band antenna.

As in Fig. 1b and c, the surface current distributions are confined to the microstrip line and the radiator. The intensity of the current is denser on the larger U-shaped patch and microstrip line than in the other places, as in Fig. 1b. In Fig. 1c, it is seen that the intensity of the current is much denser on the microstrip line and on a smaller U-shaped patch. The large U-shaped patch generates lower resonance at 2.45 GHz, and the smaller U-shaped patch generates higher resonance at 5.85 GHz. However, both the patches have a mutual influence on their resonance. Therefore, the frequencies f_1 = 2.45 GHz and f_2 = 5.85 GHz are related as $\lambda_1 \approx L_p$, and $\lambda_2 \approx 0.5L_p$, respectively, where L_p is the length of the upper U-shaped radiator, λ_0 is the free space wavelength at 2.45 GHz, λ_1 & λ_2 are the guide wavelengths. The remaining dimensions are calculated with the traditional formulae [14] and tabulated as in Table I.

TABLE I

Optimized Dimension of the Dual-Band Monopole Antenna

Parameter	W_S	L_S	W_p	L_p	W_{p1}	L_{p1}	L_f	L_g
Value, mm	0.35 λ_0	0.36 λ_0	0.125 λ_0	0.125 λ_0	0.083 λ_0	0.066 λ_0	0.183 λ_0	0.025 λ_0

The adjustable spacing between the top and lower U patches and the extent of the ground plane are the major parameters in controlling the S_{11} curve. While fabricating the antenna and soldering the connector, utmost care must be taken because the antenna is flexible and so sensitive to cables used for measurement and the copper adhesive is prone to burn while soldering. Fig. 2 demonstrates the simulated and measured S_{11} of the proposed antenna. It is observed that the reflection curve has resonance dips at 2.45 GHz and 5.85 GHz with a return loss of −12.5 dB and −18.6 dB, an impedance bandwidth of 116 MHz and 398.06 MHz, respectively. The deviation in the measured values is due to the faults in fabrication as parallax errors, while cutting the edges of the substrates, and loss factors are associated with the substrates.

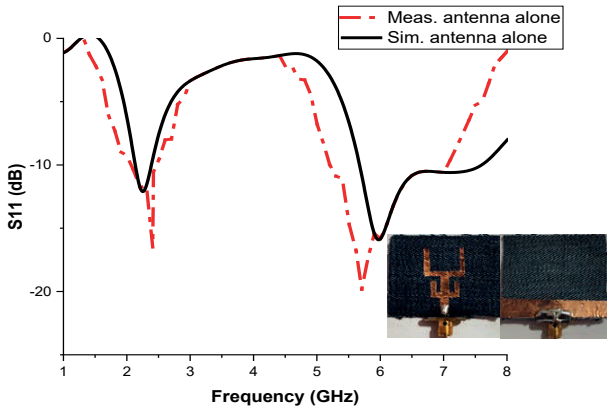

Fig. 2. Comparison between simulated and measured S_{11} curves.

B. EBG Design

The unit cell design of the proposed EBG structure comprises a simple square ring of size 28 mm × 28.5 mm. The initial square is then integrated with another square patch of size 14 mm × 14 mm, modified using slots and notches in the centre of the square ring. This is followed by the addition of triangular-shaped slits centred at each side of the outer square ring patch. The EBG structure is built on a jeans substrate of thickness h_s = 1.4 mm as shown in Fig. 3a. The dimensions of the EBG unit cell are calculated using the equations mentioned in [15], analysed and optimized through parametric simulations using CST Microwave Studio, and tabulated in Table II.

The fabricated prototype of the array of EBG unit cells is shown in Fig. 3b. Fig. 3c shows the transmission characteristics, where the proposed EBG suppresses the surface waves at the specified frequencies. The reflection phase characteristics are obtained by simulating the unit cell with periodic boundaries in both X, and Y directions using the software CST microwave studio. The structure is excited by a plane wave source placed at a distance of ten times the height of the substrate (10 h_s) on top of the EBG unit cell.

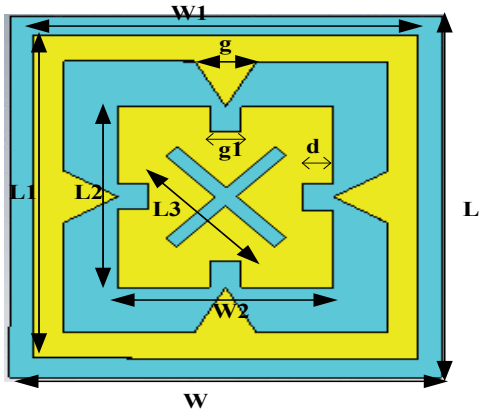

(a)

(b)

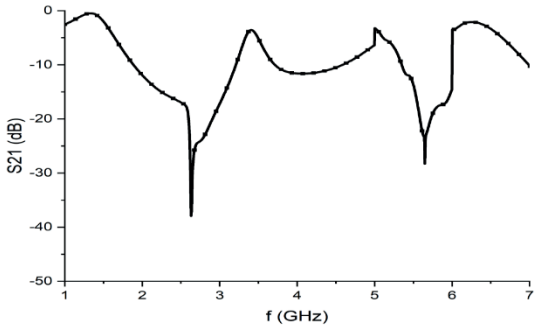

(c)

Fig. 3. (a) Geometry of proposed EBG unit cell; (b) Fabricated prototype of the proposed array of EBG unit cells; (c) Transmission characteristics of the proposed EBG structure.

TABLE II

DETAILED DIMENSIONS OF THE PROPOSED EBG UNIT CELL

Parameters	Value, mm	Parameters	Value, mm
W	28	L_3	10
W_1, L_1	25	g	4
W_2, L_2	14	g_1	2
L	28.5	d	2

Fig. 4 shows the reflection phase characteristics of the proposed unit cell. It is observed that there is a 0-degree reflection phase that appeared at 2.45 GHz and 5.85 GHz and behaved like a perfect magnetic conductor. This surface offers a high impedance of order 1.6 kΩ and 2 kΩ approximately at the specified frequencies. The EBG planes are mostly integrated into the monopole antennas that can suppress the surface by properly designing and optimizing the unit cell of EBG. This phenomenon can be visualized by simulating the array of unit cells with the suspended transmission line method. In this method, the unit cells are arranged periodically, and a microstrip line is placed above the structure. The proposed high impedance structure can suppress the surface waves at desired frequency bands, also referred to as stop bands of EBG.

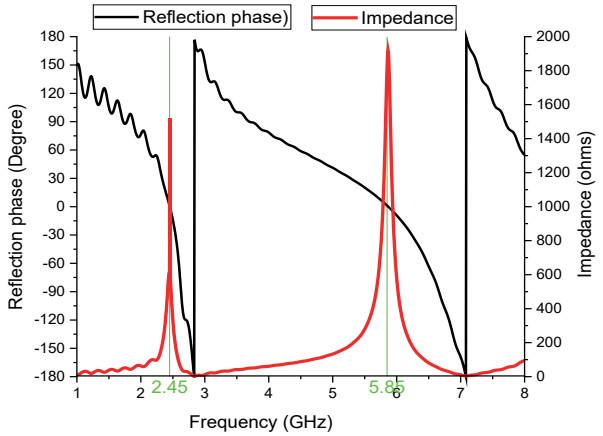

Fig. 4. Reflection phase and impedance of EBG unit cell.

C. DGS Design

Any wearable antenna design requires reducing the power loss due to back lobes and improving the radiation in the forward direction. Otherwise, they may be hazardous to humans who wear them. Therefore, critical parameter in wearable antenna design is front-to-back ratio (FBR). In general, the FBR is the ratio of power radiated in the front/main radiation lobe and the power radiated in the opposite direction (180 ° from the main beam).

$$\text{FBR} = \frac{\text{Forward Power}}{\text{Backward Power}}.$$

To improve the FBR of the wearable antenna, an EBG structure is situated at the back of the antenna. Most of the EBG structures suffer from the large size, narrow bandwidth, less radiation efficiency, and cross-polarization levels. Therefore, a novel DGS array is etched on the same substrate of EBG to alleviate the high resonant frequency, narrowband and cross-polarization level. The shape of the DGS is inspired by the traditional Dumbbell shape. Cutting a rectangular slot with four branches on all sides on the ground plane of EBG substrate forms one DGS unit cell. The characteristics of the proposed DGS array can be verified by the suspended microstrip line method, where a microstrip line is placed on the top of the substrate, and the DGS array is placed on the bottom of the substrate as the ground plane. The transmission coefficient of the proposed DGS should cover the two bands with a reference of –10 dB line. Fig. 5 shows the proposed front view of DGS array on the suspended line and surface current distribution at 2.45 GHz, and 5.85 GHz, respectively.

Observing Fig. 5b and 5c, the current distributions strongly distract the electromagnetic fields in the ground plane. In general, the slots in the ground plane distract the shielding electromagnetic fields and increase the effective permittivity of the medium. Different attributes of DGS including the shape and dimension can affect the wave propagation inside the substrate.

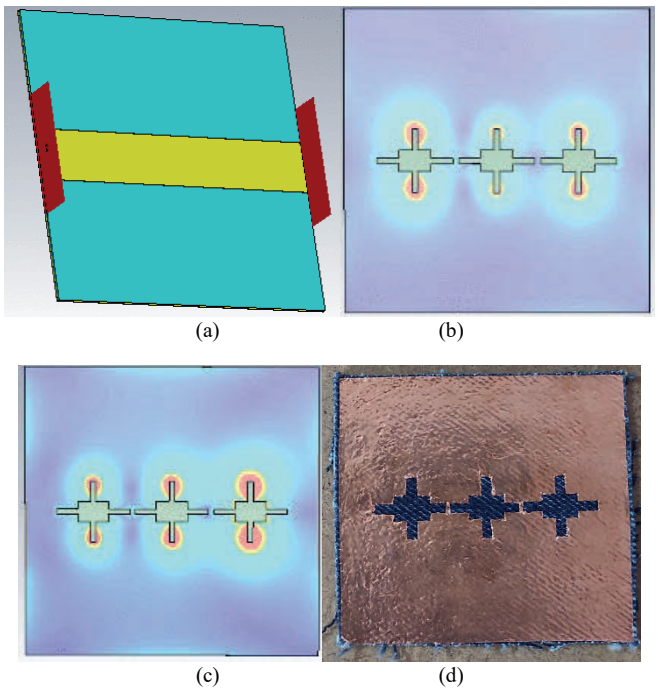

Fig. 5. (a) Suspended line method of DGS; Surface current distribution of the proposed DGS array at (b) 2.45 GHz, (c) 5.85 GHz, (d) DGS array etched on the ground plane of EBG structure.

III. Performance Analysis & Experimental Verification

The fabricated prototype of the proposed DGS integrated EBG dual-band monopole antenna and its configuration are presented in Fig. 6a, b. The monopole antenna is situated in the middle of the EBG-DGS structure, and the overall dimension of the structure is 56 mm × 57 mm × 1.4 mm. An isolated layer of foam with a 2 mm thickness is inserted between the monopole antenna and DGS loaded EBG structure to provide isolation, reducing the shorting and mismatch effects.

A. Performance of the Antenna over EBG and DGS Loaded EBG Structure

Recent wearable antenna systems necessitate a compact design with high bandwidth, radiation efficiency, and less cross-polarization levels. Therefore, DGS loaded EBG structure is introduced in this paper to improve the bandwidth and radiation efficiency, lessen the cross-polarization levels, and act as isolation between the antenna and the human body.

Situating the monopole antenna on a 2×2 array of EBG structure will detune the resonant frequency as there is a mutual coupling between the two structures. This will cause a change in the characteristics of EBG and the need to re-optimize the EBG structure to the desired resonant frequency. Further, introducing the DGS on the back of EBG also detunes the resonant frequency due to the variations of current distribution at the defects. The S-parameters of the monopole antenna alone, monopole antenna with EBG, and DGS loaded EBG structure are displayed in Fig. 6c. It is marked in Fig. 6c that the S11-parameters of monopole antenna with DGS loaded EBG structure have a better reflection coefficient at resonant

frequencies of 2.45 GHz and 5.85 GHz. It is seen that an impedance bandwidth of 115.9 MHz and 398 MHz are obtained at 2.45 GHz and 5.85 GHz, respectively. With the use of the DGS structure, the bandwidth of the final antenna is increased compared to the monopole antenna with the EBG structure. A small deviation of 1.22 % is detected between the simulated and measured reflection coefficient curves, which are due to the inhomogeneity of the flexible substrate, soldering errors, and fabrication inaccuracies.

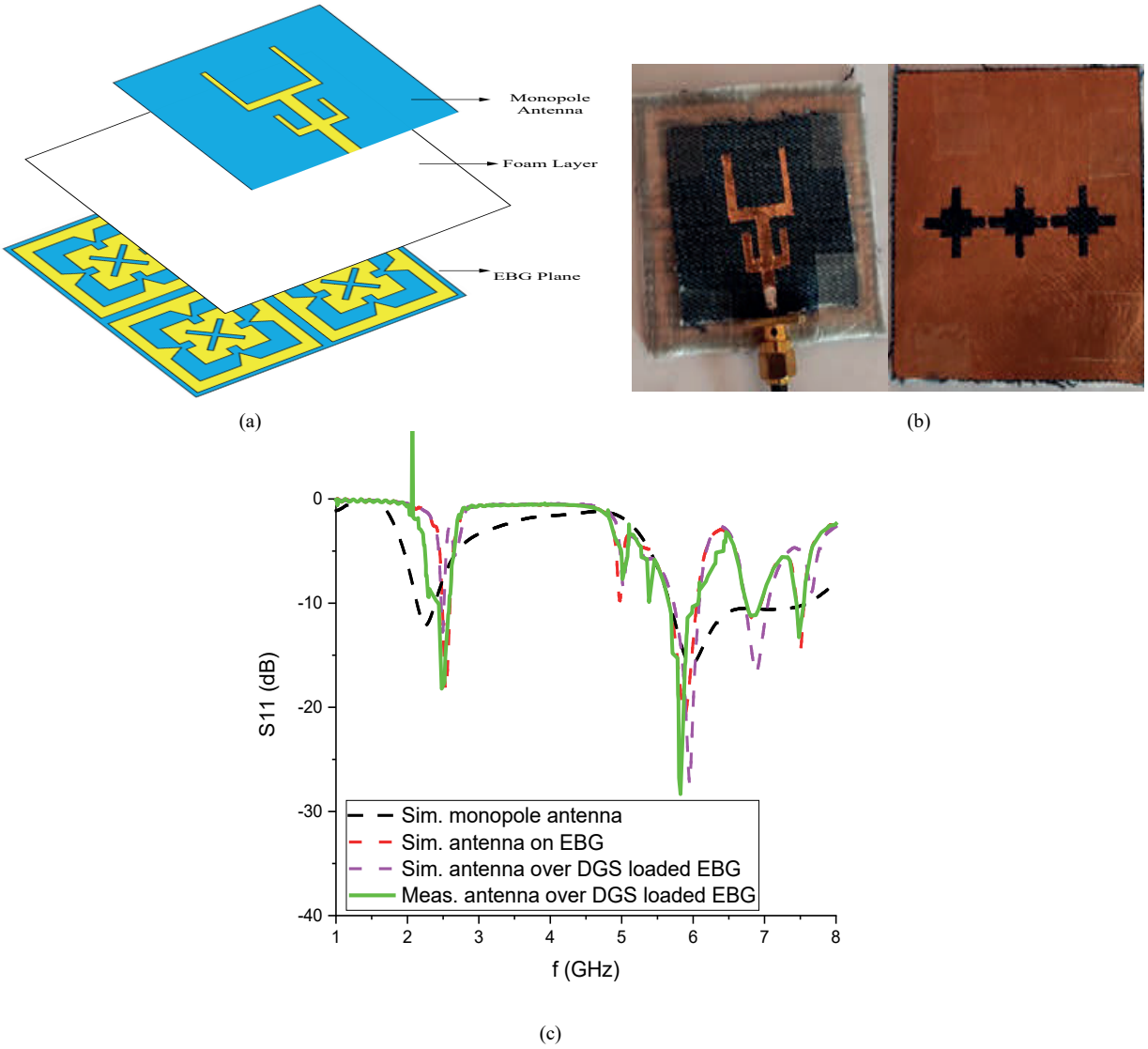

Fig. 6. (a) The configuration of the proposed antenna; (b) Fabricated prototype front and back view; (c) Reflection coefficient of the anticipated antenna.

Fig. 7 demonstrates the E-plane and H-plane radiation patterns at 2.45 GHz and 5.85 GHz; for conventional monopole antenna, the monopole antenna is integrated with EBG, and monopole antenna with DGS loaded EBG structure, respectively. The results illustrate that the E-plane radiation pattern has maximum radiation in ±Z directions; H-plane has omnidirectional patterns at 2.45 GHz and 5.85 GHz for the monopole antenna, indicating backward radiations and poor front-to-back ratio. On the other hand, backing the monopole antenna with an EBG plane, the maximum radiation is in the +Z direction and less back lobe, leading to an improved front-to-back ratio of the antenna to 10.52 dB, 28.46 dB at 2.45 GHz and 5.85 GHz, respectively. With the introduction of DGS on the ground plane of EBG, the FBR further improved to 16.77 dB and 32.72 dB at 2.45 GHz and 5.85 GHz, respectively. This is clear evidence that the radiated power in the back hemisphere of the antenna pattern is less than 6 %, 3 % at 2.45 GHz and 5.85 GHz, respectively. A substantial reduction in the back radiation is observed when integrating the antenna with EBG-DGS planes; hence, the gain is considerably improved in the broadside direction, which is most desirable in wearable applications. There is a close relation between simulated and measured values. However, small variations are due to the contribution of fabrication tolerances and soldering errors.

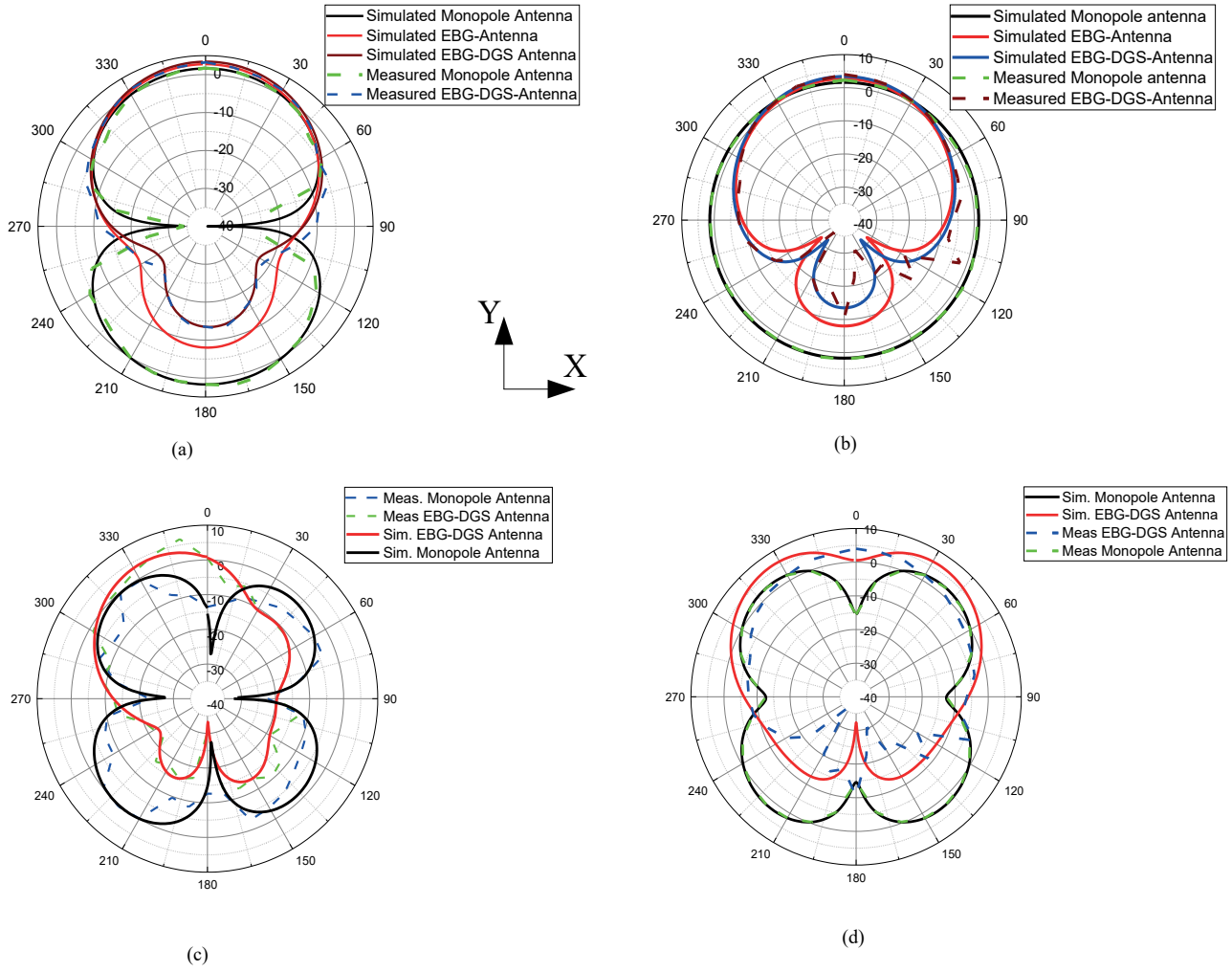

Fig. 7. Radiation patterns (a) E-plane; (b) H-plane at 2.45 GHz; (c) E-plane; (d) H-plane at 5.85 GHz.

Also, the proposed DGS disturbs the current distribution in the ground of the EBG structure and reduces the surface wave propagation. As the surface wave is reduced, the losses acquired due to surface waves are reduced, and hence the gain and radiation efficiency increase. Table III shows the comparison of gain and radiation efficiency of the monopole antenna alone and DGS loaded EBG structure. In Table III, the gain of the antenna increased to 3.37 dBi and 6.47 dBi from 1.68 dBi and 2.51 dBi, respectively, thus indicating a 50.23 % of improvement, practically doubling the gain with the usage of the DGS loaded EBG planes beneath the monopole antenna.

TABLE III

COMPARISON OF GAIN AND RADIATION EFFICIENCY OF A MONOPOLE ANTENNA, EBG BASED MONOPOLE ANTENNA, MONOPOLE ANTENNA WITH DGS LOADED EBG STRUCTURE

	Gain, dBi		Radiation Efficiency, %	
Operating frequency	2.45 GHz	5.85 GHz	2.45 GHz	5.85 GHz
Monopole antenna alone	1.68	2.51	96.60	93.11
EBG based monopole antenna	2.72	6.92	32.58	74.03
Monopole antenna with DGS loaded EBG	3.37	6.47	37.15	77.13

Fig. 8 shows the simulated co- and cross-polarization for the proposed antenna on the E, and H-plane at 2.45 GHz and 5.85 GHz, respectively. In particular rescue and emergency search and responses applications, the polarization of the

antenna can be useful for the different polarizations at the transmitter and receiver end. This can be improved by introducing the array of defects in the ground plane of the EBG structure. As the antenna is placed on X-Y (phi plane) plane, the X-Z plane is the H-plane and Y-Z plane became the E-plane. Therefore, Gain-phi plane is the co-polarization and the Gain-theta plane is the cross-polarization. It is observed in Fig. 8 that the cross-polarization level meets the low acceptable level for better antenna performance and co-polarization has the maximum main lobe magnitude in the forward direction. Also, there is better isolation observed between the co- and cross-polarization on E-plane and H-plane, respectively.

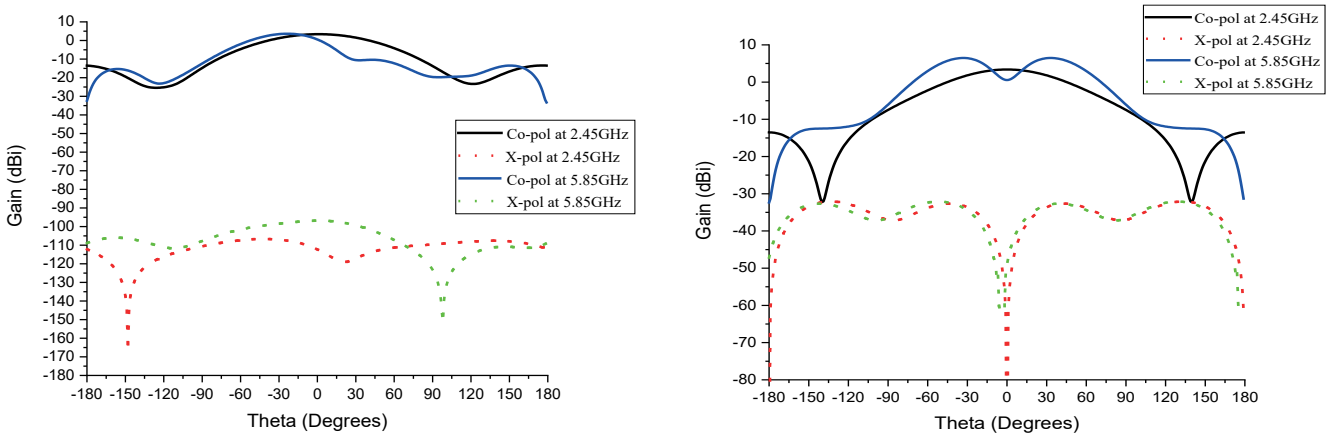

(a) (b)

Fig. 8. Simulated co- and cross-polarization of the proposed antenna in (a) H-plane; (b) E-plane at 2.45 GHz, 5.85 GHz, respectively.

B. Deformation Performance

The proposed antenna shows better performance in free space. As is it a wearable antenna, the deformation and human tissue loading should be verified with the proposed design. The proposed design is experimentally confirmed with a few radii of curvature to make certain of its flexibility and conformability. The influence of bending is verified with the use of foam cylinders of radii 70 mm and 50 mm along the E-plane and H-plane as demonstrated in Fig. 9. The radii are chosen to impersonate the parts of the human body. The design is wrapped on foam cylinders and fixed with tape.

Fig. 10 shows the reflection coefficient of the proposed design under the bending scenario. The –10 dB impedance bandwidth matching is maintained in the entire bending scenario with a slight shift in the resonant frequency. It is marked in Fig. 10 that the resonant frequency is slightly shifted under the influence of bending, still covering the desired frequencies. The radiation pattern is also verified and found that the proposed design maintains approximately the same result as that of a flat scenario, except for small variations. This investigation explores the validity of the proposed antenna under various circumstances and confirms that the anticipated antenna is useful for wearable and conformal applications in WLAN standards.

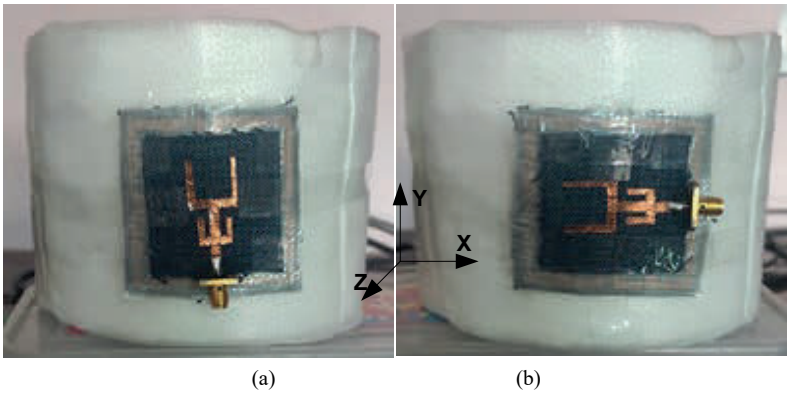

(a) (b)

Fig. 9. Photograph of the proposed antenna when wrapped around the foam cylinders of different radii R along (a) E-plane and (b) H-plane.

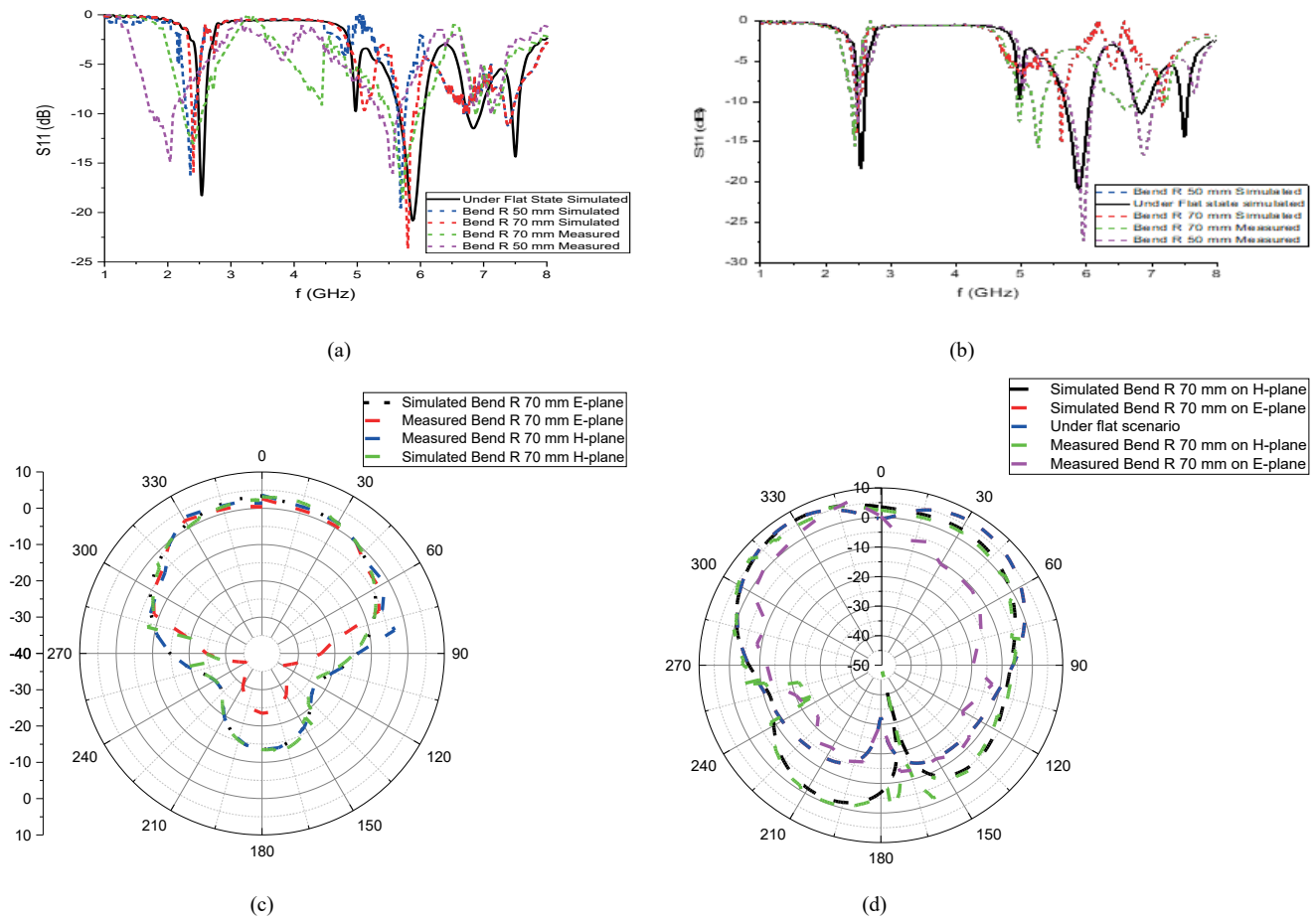

Fig. 10. Bending performance of the anticipated antenna on reflection coefficient (a) E-plane; (b) H-plane and radiation pattern at (c) 2.45 GHz; (d) 5.85 GHz.

TABLE IV

COMPARISON OF THE PROPOSED WORK AGAINST THE PREVIOUSLY PUBLISHED LITERATURE

Ref.	Year	Band of operation (GHz)	Method	Gain (dBi)	Bandwidth (%)	FBR (dB)	Overall Size (mm^3)	Substrate
[16]	2007	1.8, 2.4	Layered EBG	NA	NA	NA	119×119×4.62	Duroid 5880
[17]	2009	2.45, 5.5	EBG	NA	4, 16	15	55×55×4.48	Felt fabric
[18]	2011	2.48	Antenna surrounded by EBG	4.59	1.2	NA	65.5×81.9×1.27	ROGER3010
[19]	2013	2.45,5	suspended plate antenna	3.38, 8.33	6.95, 28.5	NA	80×100×5	Polyurethane Foam
[20]	2014	2.4, 5.5	AMC	2.5, 4	3.43, 3.45	12	100×100×4.5	Felt fabric
[21]	2015	1.8, 2.45	Fractal EBG	NA	6.94, 11.1	15	150×150×2.35	Jeans fabric
[22]	2015	1.92	AMC	4.3	8	15.8	86.5×86.5×4.8	RO4350
[23]	2016	5.15, 5.72	FSS metasurfaces	7.9, 8.2	4.09, 4.15	NA	44×44×1.75	Rogers RO4003
[24]	2018	2.45, 5.8	AMC	8.2, 9.95	NA	NA	75×50×6	Felt fabric
[25]	2019	2.5, 4.2	DGS	3.5, 5.5	NA	NA	50×40×0.8	FR4
[26]	2020	2.4	EBG-DGS	6.45	32.08	15.8	60×60×2.4	Jeans fabric
Proposed	2022	2.45, 5.85	EBG-DGS	3.37, 6.47	4.73, 16.2	16.7, 32.7	56×57×1.4	Jeans fabric

IV. Conclusion

A compact and thin, flexible textile antenna integrated with an aperiodic EBG-DGS structure has been proposed to cover the WLAN bands (2.4–2.485 GHz and 5.1–5.8 GHz) for emergency rescue applications. The design has been validated experimentally by making a prototype. The prototype covers the WLAN bands with the highest gain of 3.37 dBi and 6.47 dBi, a bandwidth of 115.9 MHz and 398.06 MHz for the specified wireless bands, respectively. A very close agreement is found between the tested and simulated values. A comparison is carried out between the monopole antenna alone and the antenna integrated with aperiodic EBG-DGS. With the integration of EBG and DGS, the isolation from the human body improved by 16.77 dB and 32.72 dB, the radiation efficiency of 36.9 % and 73.8 %, and better XP level at 2.45 GHz, 5.85 GHz, respectively. The integrated antenna exhibits a compact textile design, a thin, simple antenna with excellent isolation, cross-polarization level, great gain, and bandwidth coverage for the two specified bands compared to the reported configurations in the literature listed in Table IV. The achieved features make the proposed antenna the most appropriate and potential candidate for wearable applications in emergency search services for WLAN standards.

References

[1] F. Pervez, J. Qadir, M. Khalil, T. Yaqoob, U. Ashraf, and S. Younis, "Wireless technologies for emergency response: A comprehensive review and some guidelines", *IEEE Access*, vol. 6, pp. 71814–71838, Nov. 2018. https://doi.org/10.1109/ACCESS.2018.2878898

[2] E. F. Sundarsingh, S. Velan, M. Kanagasabai, A. K. Sarma, C. Raviteja, and M. G. N. Alsath, "Polygon-shaped slotted dual-band antenna for wearable applications", *IEEE Antennas Wirel. Propag. Lett*., vol. 13, pp. 611–614, Mar. 2014. https://doi.org/10.1109/LAWP.2014.2313133

[3] D. Kumar and D. Mathur, "Dual band wearable antenna for IoT applications", *Int. J. Innov. Technol. Explor. Eng*., vol. 9, no. 1, pp. 1515–1518, Nov. 2019. https://doi.org/10.35940/ijitee.A4344.119119

[4] S. Bhattacharjee, S. Teja, M. Midya, S. R. Bhadra Chaudhuri, and M. Mitra, "Dual band dual mode triangular textile antenna for body-centric communications", in *2019 URSI Asia-Pacific Radio Science Conference* (*AP-RASC*), Mar. 2019, pp. 1–5. https://doi.org/10.23919/URSIAP-RASC.2019.8738361

[5] M. P. Raju, D. S. Phani Kishore, and B. T. P. Madhav, "CPW fed T-shaped wearable antenna for ISM band, Wi-Fi, WiMAX, WLAN and fixed satellite service applications", *J. Electromagn. Eng. Sci*., vol. 19, no. 2, pp. 140–146, 2019. https://doi.org/10.26866/jees.2019.19.2.140

[6] S. L. Gunamony and J. B. Gnanadhas, "Design and investigations of miniaturized dual-band quarter concentric circular ring antenna for LTE and 5G applications", *Arab. J. Sci. Eng*., vol. 46, no. 10, pp. 9617–9626, 2021. https://doi.org/10.1007/s13369-021-05375-3

[7] H. Yalduz, B. Koç, L. Kuzu, and M. Turkmen, "An ultra-wide band low-SAR flexible metasurface-enabled antenna for WBAN applications", *Appl. Phys. A Mater. Sci. Process*., vol. 125, no. 9, pp. 1–11, Aug. 2019. https://doi.org/10.1007/s00339-019-2902-4

[8] C. Mao, P. L. Werner, D. H. Werner, Di. Vital, and S. Bhardwaj, "Dual-polarized armband embroidered textile antenna for on-/off-body wearable applications", in *2019 IEEE International Symposium on Antennas and Propagation and USNC-URSI Radio Science Meeting*, Atlanta, GA, USA, Jul. 2019 pp. 1555–1556. https://doi.org/10.1109/APUSNCURSINRSM.2019.8889041

[9] E. L. M. Wissem, I. Sfar, L. Osman, and J. M. Ribero, "A textile EBG-based antenna for future 5G-IoT millimeter-wave applications," *Electron.*, vol. 10, no. 2, pp. 1–12, 2021. https://doi.org/10.3390/electronics10020154

[10] F. Yang and Y. Rahmat-Samii, "EBG characterizations and classifications", *Electromagn. Band Gap Struct. Antenna Eng*., pp. 59–86, 2010. https://doi.org/10.1017/CBO9780511754531.004

[11] V. P. Kudumu and V. S. P. Mokkapati, "Reduction of surface waves in arrays using uni-planar EBG", *Int. J. Recent Technol. Eng*., vol. 8, no. 3, pp. 8065–8069, 2019. https://doi.org/10.1109/ICSPCom.2015.7150631

[12] H. Liu, Z. Li, X. Sun, and J. Mao, "Harmonic suppression with photonic bandgap and defected ground structure for a microstrip patch antenna", *IEEE Microw. Wirel. Components Lett*., vol. 15, no. 2, pp. 55–56, Feb. 2005. https://doi.org/10.1109/LMWC.2004.842809

[13] M. Wang *et al*., "Investigation of SAR reduction using flexible antenna with metamaterial structure in wireless body area network," *IEEE Trans. Antennas Propag*., vol. 66, no. 6, pp. 3076–3086, Mar. 2018. https://doi.org/10.1109/TAP.2018.2820733

[14] B. C.A, "Antenna Theory_ Analysis and Design (1996).pdf." .

[15] D. Sievenpiper, L. Zhang, R. F. Jimenez Broas, N. G. Alexöpolous, and E. Yablonovitch, "High-impedance electromagnetic surfaces with a forbidden frequency band", *IEEE Trans. Microw. Theory Tech*., vol. 47, no. 11, pp. 2059–2074, Nov. 1999. https://doi.org/10.1109/22.798001

[16] X. Wang and Y. Hao, "Dual-band operation of an electromagnetic band-gap patch antenna", *Microw. Opt. Technol. Lett*., vol. 49, no. 11, pp. 2562–2568, Jul. 2007. https://doi.org/10.1002/mop.22728

[17] S. Zhu and R. Langley, "Dual-band wearable textile antenna on an EBG substrate", *IEEE Trans. Antennas Propag*., vol. 57, no. 4, pp. 926–935, Apr. 2009. https://doi.org/10.1109/TAP.2009.2014527

[18] R. C. Hadarig, M. E. De Cos, and F. Las-Heras, "Microstrip patch antenna bandwidth enhancement using AMC/EBG structures", *Int. J. Antennas Propag*., vol. 2012, Art no. 843754, 2012. https://doi.org/10.1155/2012/843754

[19] N. Husna *et al*., "Dual-band suspended-plate wearable textile antenna", *IEEE Antennas and Wireless Propagation Letters*, vol. 12, pp. 583–586, Apr. 2013. https://doi.org/10.1109/LAWP.2013.2259211

[20] S. Yan, P. J. Soh, and G. A. E. Vandenbosch, "Low-profile dual-band textile antenna with artificial magnetic conductor plane", *IEEE Trans. Antennas Propag*., vol. 62, no. 12, pp. 6487–6490, Sep. 2014. https://doi.org/10.1109/TAP.2014.2359194

[21] S. Velan *et al*., "Dual-band EBG integrated monopole antenna deploying fractal geometry for wearable applications", *IEEE Antennas Wirel. Propag. Lett*., vol. 14, pp. 249–252, Apr. 2015. https://doi.org/10.1109/LAWP.2014.2360710

[22] T. Andriamiharivolamena, P. Lemaître-Auger, S. Tedjini, and F. Tirard, "Compact planar monopole antenna for wearable wireless applications", *Comptes Rendus Phys*., vol. 16, no. 9, pp. 851–861, Nov. 2015. https://doi.org/10.1016/j.crhy.2015.07.008

[23] H. Yang, W. Yao, Y. Yi, X. Huang, S. Wu, and B. Xiao, "A dual-band low-profile metasurface-enabled wearable antenna for WLAN devices", vol. 61, pp. 115–125, Jan. 2016. https://doi.org/10.2528/PIERC15092803

[24] A. Mersani, L. Osman, and J. M. Ribero, "Performance of dual-band AMC antenna for wireless local area network applications", *IET Microwaves, Antennas Propag*., vol. 12, no. 6, pp. 872–878, May 2018. https://doi.org/10.1049/iet-map.2017.0476

[25] B. P. Nadh, B. T. P. Madhav, and M. S. Kumar, "Design and analysis of dual band implantable DGS antenna for medical applications", *Sadhana - Acad. Proc. Eng. Sci*., vol. 44, no. 6, pp. 1–9, May 2019. https://doi.org/10.1007/s12046-019-1099-8

[26] A. Y. I. Ashyap *et al*., "Robust and efficient integrated antenna with EBG-DGS enabled wide bandwidth for wearable medical device applications," *IEEE Access*, vol. 8, pp. 56346–56358, 2020. https://doi.org/10.1109/ACCESS.2020.2981867

Sandhya Mallavarapu is currently pursuing her PhD in Electronics and Communications Engineering at the National Institute of Technology Warangal. She received her M. Tech degree in Communications and Signal Processing from R.V.R & J.C, Guntur, Andhra Pradesh, India in 2013 and B. Tech degree in Electronics and communications engineering from Vignan's Engineering College, Guntur, Andhra Pradesh, India in 2010. Her research interests include flexible and wearable multi-band antennas. She has two international conference papers and two papers in various journals indexed in SCI/ESCI to her credit.
E-mail: sandhyamallavarapu@student.nitw.ac.in
ORCID iD: https://orcid.org/0000-0002-1899-2955

Anjaneyulu Lokam was born in 1967, in India. He received his B. Tech (ECE) in 1989, M. Tech in 1991, and PhD in 2010 from N.I.T, Warangal, and Telangana, India. He worked as a Project Officer at the Institute of Armament Technology, Pune, India, for five years from 1991 and was involved in the Design of Surface Borne and Air Borne Radar Systems for Clutter Measurement Applications. Later, he worked as a Staff Scientist at Helios Systems, Madras, India, for two years and developed Radio Wave Propagation Assessment Software Modules for Ship-borne Radars. He has been with the Department of Electronics and Communications Engineering at the National Institute of Technology, Warangal, India, since 1997. His area of interest includes Computer Networks, Electromagnetic Field Theory, Microwave, and Radar Engineering, Microwave Remote Sensing, and Neural Networks & Fuzzy Logic Systems. He has completed few defence-related R&D projects and has 100 papers to his credit in national and international conferences and journals. He is a life member of ISTE and a member of IEEE, IEEE antennas and Propagation Society, IEEE signal processing society.
E-mail: anjan@nitw.ac.in
ORCID iD: https://orcid.org/0-0001-7709-4365